Atherosclerosis Plaque Neovascular Inflation Using Ultrasound Strain Imaging

Canxing Xu

A thesis
submitted in partial fulfillment of the
requirements for the degree of
Master of Science

University of Washington
2014

Committee:
Chun Yuan (chair)
Kirk W. Beach
Jeff Powers
Pierre D. Mourad

Program Authorized to Offer Degree:
Bioengineering

University of Washington

Abstract

Atherosclerosis Plaque Neovascular Inflation
Using Ultrasound Strain Imaging

Canxing Xu

Chair of the Supervisory Committee:
Dr. Chun Yuan
Department of Bioengineering

Vasa vasorum (VV) are small arterial and venous networks that originate from major arteries and drain into major veins; penetrating into the arterial wall to supply oxygen and nutrition for the tissues on the outer layer of the vessel walls and draining the by-products of metabolism. In the case of atherosclerosis, VV may grow into the plaque and supply the cells inside, which contribute to the progression of atherosclerosis and increase the risk of future plaque rupture. Additionally, VV could also be a source of intraplaque pressure that inflates the plaque when the luminal pressure decreases below a certain threshold during the cardiac cycle. Such cyclic inflations could pose another risk factor of a vulnerable plaque as the dynamics during inflations could weaken the caps of plaque. A sudden change between the intraplaque pressure and the luminal pressure would incur more inflation stress on the plaque cap and thus increase the

likelihood of plaque rupture. Therefore, the density of VV within an atherosclerotic plaque could be an important factor to estimate the vulnerability.

Ultrasound strain imaging is a technique that can be used to measure non-invasively how much a plaque inflates during a cardiac cycle, which could be associated with the volume of VV inside the plaque. In addition, the peak-systolic velocity (PSV) within the stenosis affects the plaque inflation due to the Bernoulli Effect.

The work in the thesis focuses on a pilot study to research how the carotid plaque inflates among carotid atherosclerosis patients with ultrasound strain imaging, and relates the inflation with the PSVs measured by spectral Doppler. 22 carotid stenosis cases were studied and the results show that most carotid plaques inflate during cardiac cycle, and inflations correlate with PSV. The results provide encouraging evidence to the VV inflation hypothesis and pave the path to future in-depth research on larger population of patients.

Contents

1. Introduction

Stroke is one of the leading causes of death in the United States (following coronary heart disease and cancer) and it is a large burden to the society. By estimation, the direct healthcare cost of stroke was $22.8 billion in a single year of 2009. In the U.S., about 795,000 people experience a new or recurrent stroke each year. Around 87% of them are ischemic stroke [Go, 2013], which is closely related with the severity of carotid atherosclerosis [Honda, 1995]. There is need to establish reliable metrics to evaluate vulnerable carotid plaques to effectively select vulnerable patients for surgery and intervention and to reduce the onset of stroke.

Research on vulnerable atherosclerosis has been focused on the composition of plaques. It is believed that plaques with large lipid core and intraplaque hemorrhage are prone to rupture, while fibrous plaques tend to be more stable [Naghavi 2003]. Recent research and clinical studies also implicate the essential role of the vasa vasorum (VV) in vulnerable plaques [Langheinrich 2007]. In large arteries, oxygen and nutrient supply of the intima and inner media are provided by the luminal blood diffusion, while the outer media and the adventitia layers are supplied by additional small vessel networks of the VV. VV typical originates from other arteries near the major arteries. The VV supplying the carotid arteries, for example, originates from the ascending pharyngeal artery [Bo 1989].

When there is a plaque, VV could penetrate the normal arterial wall and enter the plaque to provide nutrition to the abnormal cells there. A high density of VV is often found in the ruptured plaques. Also, the high density of VV could contribute to the formation of the lipid core and the breakdown of elastic fiber around the plaque, leading to a thin fibrous cap of plaques [Virmani 2005].

This thesis also focuses on the VV in vulnerable plaques. Instead of the role of VV in plaque composition and progression, however, we focused more on the mechanical effect that VV contributes to the rupture of plaques.

VV inside the plaque must be a major source of intraplaque pressure that causes the plaque to inflate at a certain phase of each cardiac cycle when the luminal pressure is below the blood pressure from VV. Such cyclic inflation might weaken the cap of plaque, and, if an extreme condition suddenly changes the pressure difference between two sides, the stress of the cap would increase and it could be blown off and cause embolic events like stroke. This hypothesis has been suggested by John Johnson in 1980. He suggested that the rupture of a plaque might be akin to the eruption of Mt. St. Helens, where lava kept flowing into the bottom of the volcano and the internal pressure continued to increase until exceeding the limit of its top and thus erupting.

Based on this hypothesis, there are two relevant risk factors for an atherosclerotic plaque to rupture due to transmural pressure difference. As indicated in Fig. 1-1, the two factors are: 1) high intraplaque pressure P_i, and 2) reduced luminal pressure P_o.

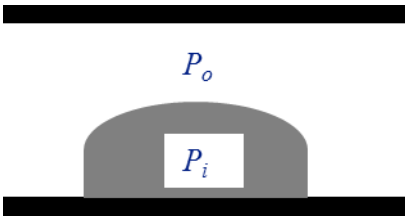

Figure 1-1. Pressures around the plaque. Black bars stand for the artery walls, and the gray area is the plaque. P_o is the luminal pressure, and P_i is the intraplaque pressure.

The first risk factor, intraplaque pressure from VV, is difficult to measure directly. Intraplaque VV volume can be used as an alternative risk factor. Although it might not be necessarily proportional to the intraplaque pressure, higher VV volume could result in higher magnitude of

cyclic plaque inflation and deflation, and thus higher risk of fibrous cap weakening and rupture. Magnetic Resonance Imaging (MRI) [Kampschulte 2004 and Takaya 2005] and ultrasound contrast-agent imaging [Carlier 2005 and Staub 2010] have shown the potential in detecting the existence and density of VV inside atherosclerosis. However, MRI examination is costly, while ultrasound with contrast agent is considered as an invasive modality and it is also relatively expensive. Alternatively, ultrasound strain / elastography imaging [Gao 1996 and Greenleaf 2000] can be used to estimate the volume of intraplaque VV noninvasively by measuring how much a plaque inflates during each heart cycle.

Based on motion and speckle tracking, ultrasound strain imaging can be used to measure several strain waveforms, including the luminal diameter, the arterial wall thickness, and the plaque thickness. By tracking the motion of the arterial walls and the top of a plaque, as shown in Fig. 1-2(a), the arterial diameter strain waveform and the plaque thickness strain waveform can be measured.

The arterial diameter strain is calculated as:

$$\frac{[d_2(t) - d_1(t)] - [[d_2(0) - d_1(0)]}{d_2(0) - d_1(0)} \times 100\%$$

The plaque thickness strain is calculated as:

$$\frac{[d_2(t) - d_3(t)] - [[d_2(0) - d_3(0)]}{d_2(0) - d_3(0)} \times 100\%$$

where t is the time variable and t = 0 is defined as the first QRS trigger. d_1 and d_2 are the displacement of the arterial walls, while d_3 is the displacement of the cap of the plaque.

The arterial wall diameter changes as the luminal pressure pulses during cardiac cycles, as the blue waveform shown on top of Fig. 1-2(b). Ideally, the arterial diameter waveform should have the same shape as the luminal pressure waveform, while the thickness waveform of a normal vessel wall or a plaque with only elastic materials would be inversely proportional to the trend of luminal pressure, as the red waveform in Fig. 1-2(b). In case of VV, we believe that the range of intraplaque blood pressure from VV should lie between the systolic and diastolic pressure inside the lumen. Thus, blood will have chance to enter the plaque when the transmural pressure is higher in the plaque side and be squeezed out of the plaque when the luminal pressure is higher. Therefore, we expect to see an excess inflation in plaque strain waveform when the intraplaque pressure is higher and VV supply nutrients to the plaque, as the magenta waveform in Fig. 1-2(b). The amount of inflation should correspond to the volume of VV.

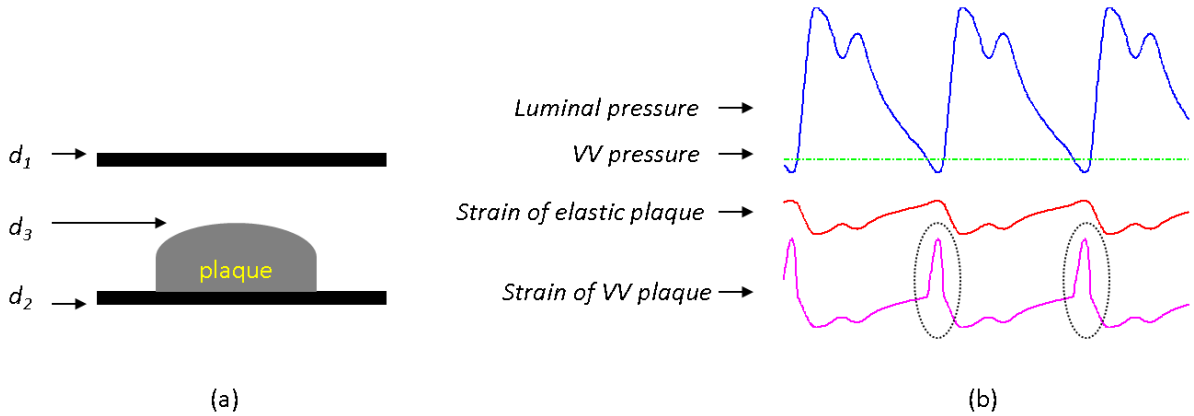

Figure 1-2. (a) The displacement of several points of interests (POIs) inside a carotid segment with plaque: d1 – displacement of the near wall, d2 – displacement of the far wall, d3 – displacement of the plaque top; (b) The relationship between the pressures and the plaque strain. The waveform on top is the normal pressure waveform inside the carotid during several cardiac cycles. The green dash line indicates the hypothetic VV pressure. The red waveform below is an expected strain waveform of a plaque with only elastic or stiff materials. The magenta waveform on the bottom is an expected strain waveform of a plaque with VV. The black dashed circles include the moment that the plaque inflates as the intraplaque pressure from VV is higher than the luminal pressure.

The second risk factor of reduced luminal pressure relates to the increased blood flow velocity around the stenotic regions. Due to the Bernoulli Effect, the pressure depression is estimated as:

$$\Delta P = 4V^2$$

where V is the flow velocity in meters per second, and P is in mmHg [Beach 1993]. A high stenotic velocity about 300 cm/s could result in a pressure drop of up to 36 mmHg, which is almost a 30% reduction compared to normal systolic pressure.

Therefore, high flow velocity in the stenotic region could potentially increase the risk of plaque rupture by reducing the luminal pressure and thus increasing the transmural pressure difference. Following the convention, Doppler spectra can be used to measure the PSV and hence the pressure depression at the site of stenosis [Hatle 1978 and 1980].

2. Significance

The long term goal of this research is to establish a correlation between the density of VV and vulnerable plaques, and recommend a non-invasive ultrasound method to measure the density of VV for reliable vulnerable plaque screening.

As the initial step, this thesis work focused on a pilot study that measured the inflation of plaque using an ultrasound strain imaging technique from a small number of carotid atherosclerotic patients, and correlated the inflation with the size of stenosis and the blood velocity. In this preliminary stage, no "gold standard" like MRI or contrast-agent imaging was used. We expect this pilot study would find some evidence about plaque inflation and build the foundation to conduct in-depth study on a larger number of patients.

3. Method

3.1 Data Acquisition

Twenty patients visiting the Department of Surgery at University of Washington Medical Center were recruited as the subjects of this study. Each subject had at least one atherosclerotic plaque on one or both sides of the carotids. All stenotic carotids among these subjects were scanned by an experienced sonographer according to an approved University of Washington IRB protocol. Altogether, thirty carotid artery examinations were collected from these subjects. During data analysis, eight cases were discarded due to bad ECG triggers or poor signal to noise ratio in the ultrasound data, leaving a total of twenty-two valid cases for further analysis.

The ultrasound scanner used in this study was a Hi Vision 5500 system (Hitachi Medical System America, Twinsburg, OH, USA) with an EUP-L53 linear-array transducer centered at 7.5 MHz. This system provided academic customers a research interface to capture a series of ultrasound frames in quadrature demodulated IQ format. The datasets collected for each case consisted of several BW sequences with narrowed width, multiple Doppler spectra, and ECG trigger signals. Since the frame rate is essential to estimate the arterial wall motions accurately, the width of the BW frames was reduced to the system minimum to achieve the highest possible frame rate, which is 271 Hz under the minimal width of the scanner. In order to cover the area of interest, several min-width datasets were collected around the stenotic region from proximal to distal in each case. Figure 3-1 shows an overview of a stenotic carotid on a BW image with normal scanning width, and 4 different min-width datasets and their relative locations with regard to the overview BW image. Depending on the size of the plaque, four to nine datasets were collected

for each case. In terms of time duration, each dataset contains up to 1,000 frames, covering about two to three complete cardiac cycles.

The Doppler spectra were acquired simply by performing screen capture on the ultrasound scanner during the exam, as shown in Fig. 3-2. Based on the screenshot, peak-systolic velocity (PSV) was estimated from the measured peak velocity in each spectrum and angle-corrected manually (i.e., obtaining the true PSV by factoring out the angle between the blood flow and the ultrasound beam). In the spectrum shown in Fig. 3-2, the angle between the ultrasound beam and the blood flow direction is about 60 degrees, while the measured PSV from the spectrum is around 55 cm/s, thus the true PSV after angle correction will be:

$$\frac{55\ cm/s}{\cos(60°)} = 110\ cm/s$$

To capture the jet velocity, multiple Doppler spectra from different angles were acquired on or near the stenotic regions. The maximal PSV from all angle-adjusted Doppler spectra in each case was selected as PSV of the case.

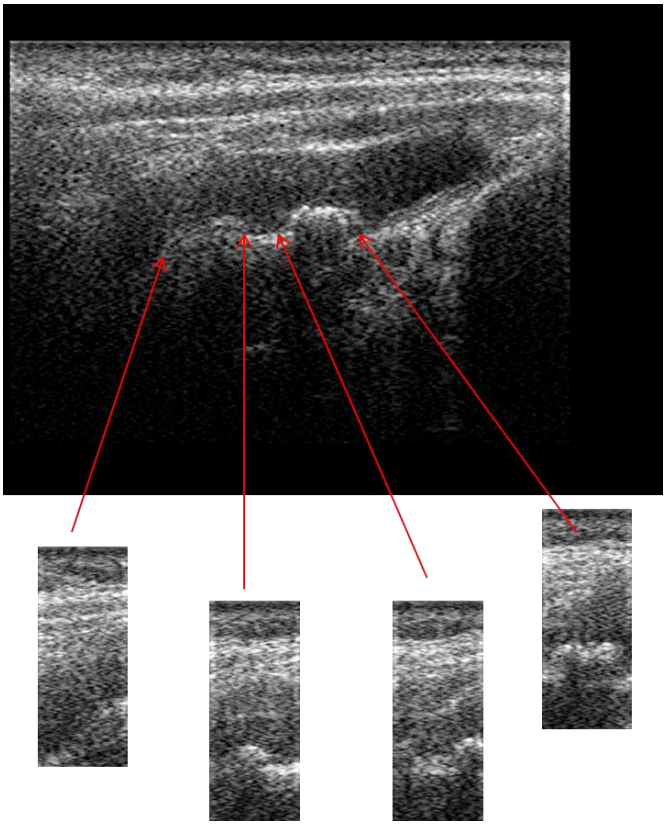

Figure 3-1. Narrow-width BW frames around the carotid stenosis and their relative position in regard to the wide BW frame

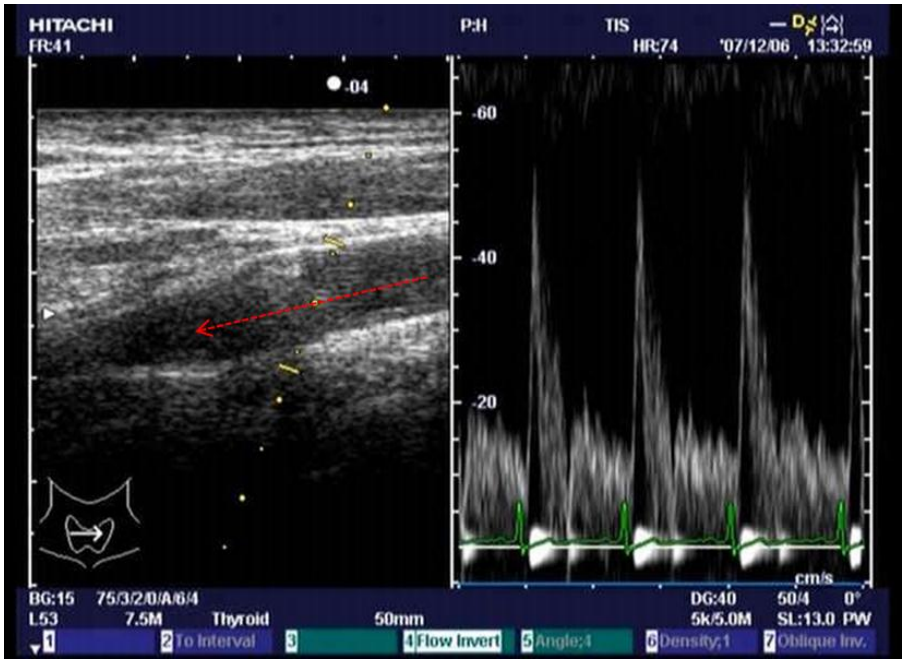

Figure 3-2. Screenshot of a Doppler spectrum. Note that the angle between the ultrasound beam (yellow dashed line) and the approximate blood flow direction (red dashed arrow) is about 60 degrees. Given the measured PSV of 55 cm/s from the spectrum, the angle corrected PSV is 110 cm/s in this case.

3.2 Arterial Wall Motion and Strain

Before measuring the arterial wall motion and strain, the experienced sonographer sketched the inner layers and outer layers of both arterial walls (near wall and far wall) on the first frame of each min-width dataset, as shown in Fig. 3-3. In case of an atherosclerosis plaque, it is just enclosed by the inner layer and the outer layer of the wall where it is attached.

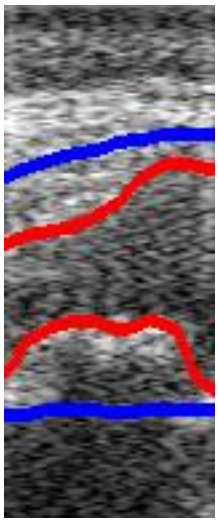

Figure 3-3. Manually-sketched arterial walls (red of inner layers and blue for outer layers). Part of a plaque is covered by the inner and outer layer on the far wall.

The sketched profiles were also used to estimate the percent stenosis roughly by the percent ratio of the plaque thickness to the diameter of the outer walls. The largest stenosis ratio among all the datasets for the artery was selected as the percent stenosis of the case.

After the arterial walls were marked by the sonographer, the axial motion of each point along the walls was tracked and recorded across at least two complete cardiac cycles. The method used to estimate the motion at one point between two consecutive frames was the phase-based auto-correlation method [Rabben 2002 and Shamdasani 2007] that operates on the complex IQ data.

After obtaining the motion data, three types of waveforms about the arteries/plaque motion or strain were derived:

- *Diametric/thickness change waveform*. It represents the change of the diameters of the vessel lumen or the thickness of the walls. For instance, the diameter change waveform of the inner lumen is calculated by subtracting the motion of the inner far wall with the motion of the inner near wall over time.
- *Strain waveform*. It reflects the relative change of arterial diameters or the wall/plaque thickness over time, equivalent to the diametric/thickness change waveform divided by the original diameter/thickness at the QRS signal trigger.
- *Diametric/thickness change rate waveform*. This waveform depicts how fast the diameter/thickness changes. Positive values stand for the speed of inflation, while the negative values represent the deflating rate. Theoretically, it is equivalent to the temporal derivative of *diametric/thickness change waveform*, but it might have a potential advantage over the diametric/thickness change waveform. Because the change rate waveform is just derived from the motion between two consecutive frames but the diametric/thickness change waveform is computed by accumulating the frame-to-frame motions over time, the diametric/thickness change waveform is more sensitive to the bias during motion estimation, as the motion bias could be accumulated over time.

Finally, quantitative metrics to describe how much the arterial wall or the plaque inflates during the cardiac cycles were developed from these waveforms. The correlation between the metrics and PSV or the percent stenosis was analyzed to evaluate whether the inflation of the plaque is related to the Bernoulli pressure drop inside the lumen or the size of the plaque.

4 Results

4.1 Strain waveforms

Figure 4-1 shows the strain waveforms of a segment of normal carotid artery without atherosclerosis. In Fig. 4-1(a), the min-width BW frame of the carotid segment is shown with the marked intima and adventitia layers of both the near and the far walls.

The diameter/thickness waveforms are shown in Fig. 4-1(b). Each waveform typically covers two complete cardiac cycles, starting from the first QRS trigger in the dataset, and stopping at the third QRS trigger, with the second trigger shown as the vertical dash line in the middle. Positive values of the waveforms stand for inflation, while negative values represent deflation. Corresponding to the color scheme in Fig. 4-1(a), the red waveform stands for the diameter change of the artery between the two inner walls, the blue waveform is the diameter change between the two outer walls. The thickness change of the near wall and the far wall are shown with color green and magenta, respectively, corresponding to the green and magenta arrows in Fig. 4-1(a). From the diameter/thickness waveforms, the strain waveforms were also created by converting the waveforms from Fig. 4-1(b) into the percentage ratio of their original diameter/thickness at the first QRS trigger, as shown in Fig. 4-1(c).

A third group of waveforms is the thickness change rate waveform (mm/s), which depicts how fast the wall inflates or deflates. It can be considered as the derivative of the thickness change waveform in Fig. 4-1(b). As shown in Fig. 4-1(d), the color scheme is also similar to the other waveforms: green for the near wall and magenta for the far wall. The change rate waveforms of the wall diameter are not shown in the result since they are of less interest.

In addition, one of the Doppler spectra within the location of the narrow BW frame is also included to check if the PSV is normal (Fig. 4-1(e)). In this case, the measured PSV waveform is about 20 cm / s. With a Doppler angle about 60 degrees, the angle-adjusted PSV is 40 cm /s.

As an example of a normal carotid segment, the waveforms shown in Fig. 4-1 match the prediction well. The diametric change waveforms (red and blue in Fig. 4-1(b) and 4-1(c)) correspond with the typical arterial pressure waveform inside the carotid (see Fig. 1-2). They both show a rapid rise of pressure at the beginning of systole and reach the systolic peak, a dicrotic notch related to the closure of the aortic valve, and a slower decrease during diastole. In contrast, the arterial wall thickness waveforms (green and magenta in Fig. 4-1(b) and 4-1(c)) show exactly the opposite trend to the diametric waveforms, also as predicted. Also note that the strain waveforms of the wall thickness are nearly the inverse of the strain waveforms of the diameters. This also matches the prediction as the cross section of the arterial wall is π*diameter*thickness. With the assumption of constant cross section, a 5% increase in diameter should result in a 5% decrease in wall thickness.

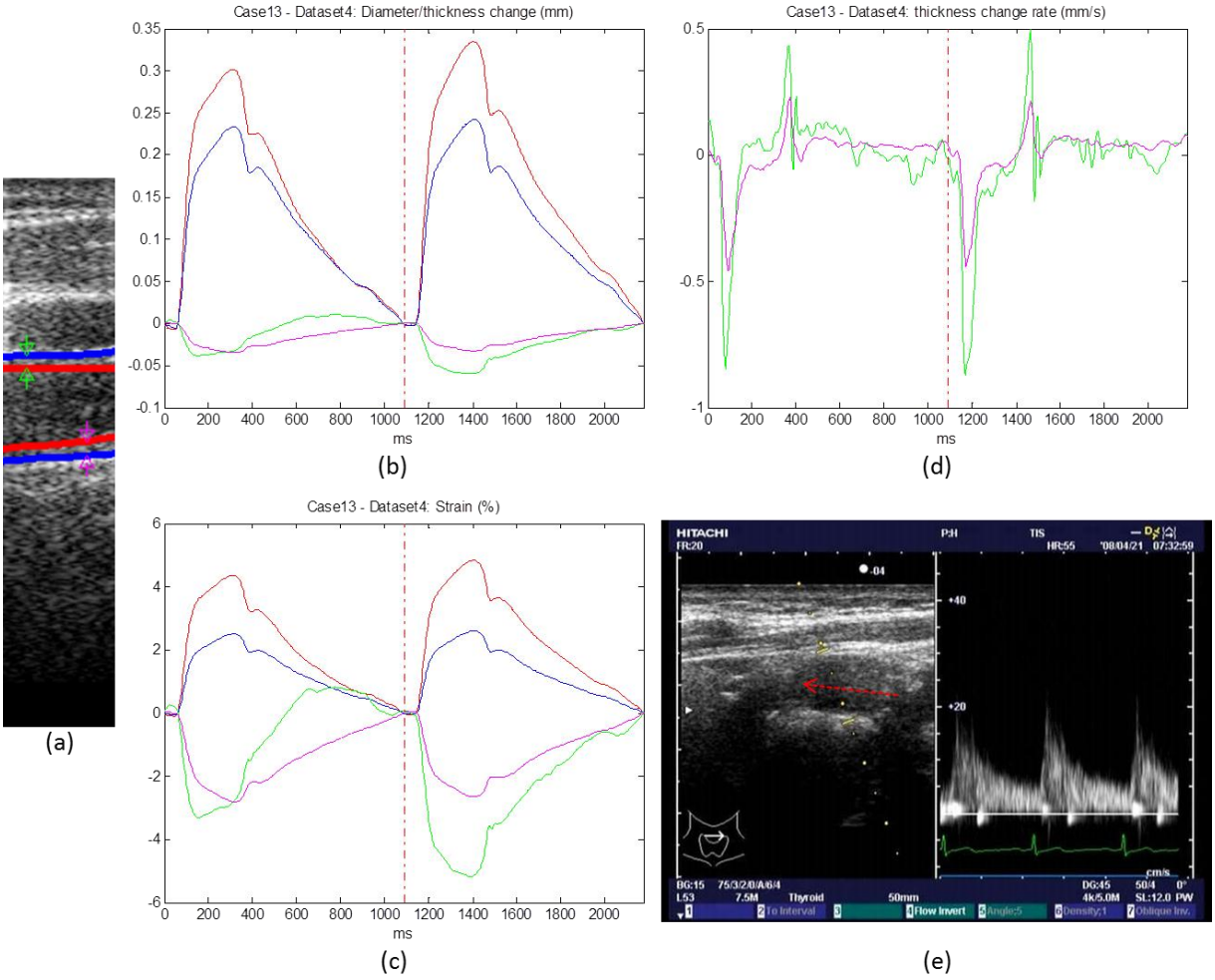

Figure 4-1. Arterial wall strain waveforms of a normal carotid segment: (a) the carotid segment with the wall markers; (b) the diameter/thickness change waveform (unit: mm). Red: waveform of the near wall (intima & limen) diameter change; Blue: waveform of the far wall (adventitia) diameter change; Green: waveform of the superficial (near) wall thickness change; Pink: waveform of the (far) deep wall thickness change. The waveforms cover 2 cardiac cycles with the start time and end time of QRS triggers, and the dash line indicate the QRS signal in the middle. (c) The strain waveforms with the same color scheme of (b). (d) The thickness change rate waveforms (unit: mm/s), with the same color scheme of (b). (e) The Doppler spectrum on the region of interest, with a measured PSV of 20 cm/s and a Doppler angle of 60 degree.

Figure 4-2 shows the waveforms of a segment of stenotic carotid artery with a plaque on the near wall. In Fig. 4-2(b) and 4-2(c), it can be seen that both the diameter waveforms (red and blue) and the far wall thickness waveform (magenta) behave similarly like a segment of normal carotid artery. That is, the diameters inflate while the wall thickness deflates during systole. However, the thickness waveform of the near wall (green) with a small plaque behaves complete opposite

to the stenosis-free far wall. It inflates just like the diameter waveform. This is a type of waveform that is expected to be seen when there is an intra-plaque pressure from VV in addition to the luminal pressure drop due to high PSV. In this example, the PSV is 120 cm/s, slightly above the normal.

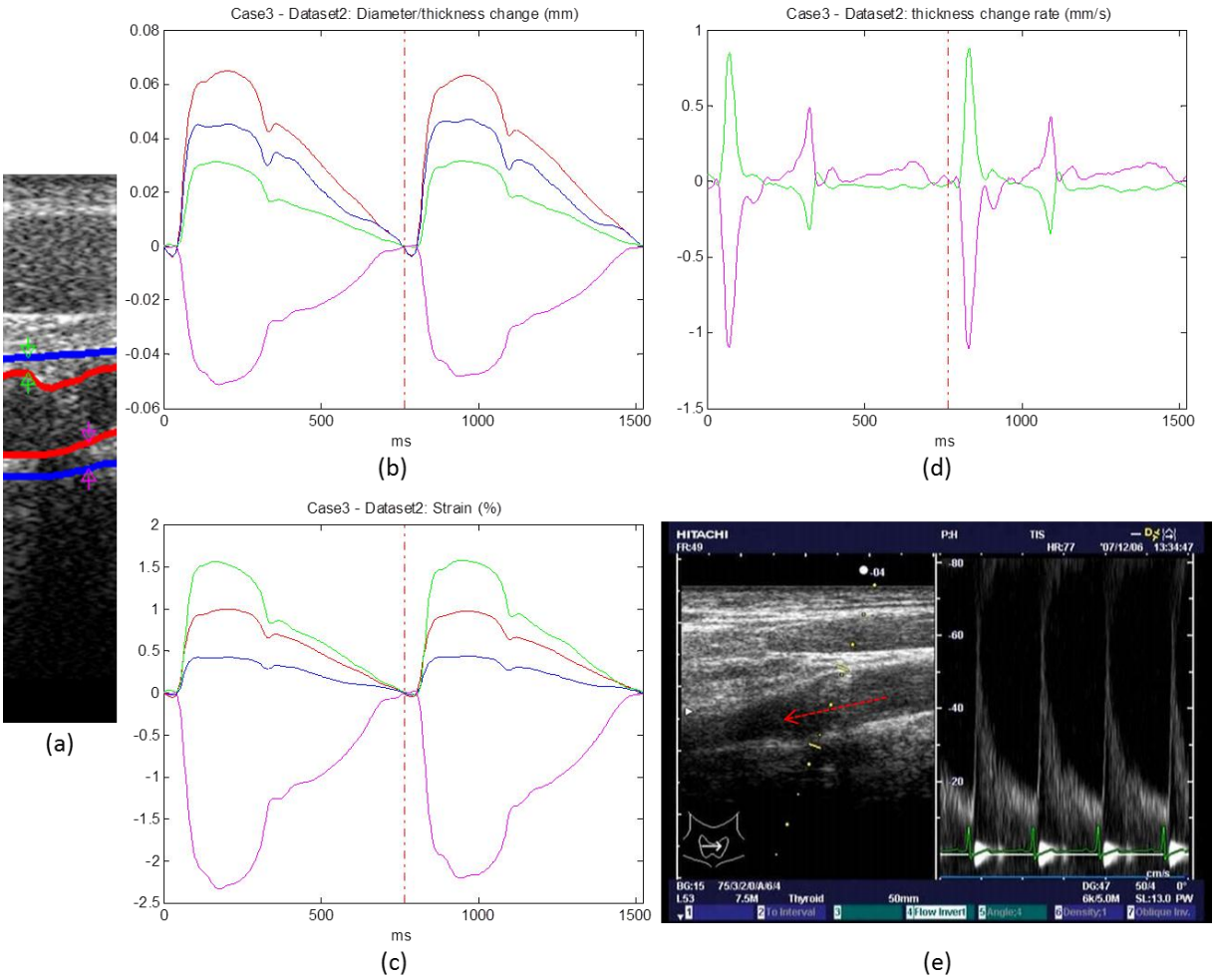

Figure 4-2. The arterial wall strain waveforms of a stenotic carotid segment. (a) The min-width BW frame with the arterial wall markers show a stenotic plaque on the near wall of the arterial; (b) The thickness change waveform shows inflation of the plaque on the near wall (green); (c) The strain waveform also indicates inflation of the near wall plaque (green); (d) The thickness change waveform shows an increase in plaque inflation speed (green); (e) The doppler spectrum. A measured PSV of 60 cm/s and Doppler angle of 60 degree give an angle-adjusted PSV of 120 cm/s

Figure 4-3 shows another example of stenotic carotid artery. In this case, both the near wall and the far wall have atherosclerotic stenosis plaques, as shown in Fig. 4-3(a). From the diameter/thickness change and strain waveforms in Fig. 4-3(b) and 4-3(c), the artery diameter waveforms still show the same pattern as the normal carotids. However, the thickness waveforms of the plaques on both walls exhibit an inflation pattern during the cardiac cycle, which is complete opposite to the behavior of wall thickness change of a normal carotid. This could imply the effects of VV pressure on both walls, in addition to a pressure drop due to high PSV, which is 170 cm/s in this case.

In the case of severe stenosis, it is possible that the pressure drop due to high jet velocity is so large that the arterial lumen or/and the arterial diameters actually decrease during systole. As the examples shown in Figs. 4-4 and 4-5, both carotids are greatly narrowed by large plaques on both walls. As many other cases, the plaques inflate during systole (the green and magenta waveforms). But the luminal size, which is the inner wall diameter, decreases at peak systole (the red waveforms) in both cases. In the example shown in Fig. 4-5, even the outer wall has a negative peak-systolic diameter change. These findings are completely consistent with the expectation in case of severe stenosis. Surprisingly, the measure PSV in both cases is not very high. It is 160 and 100 cm/s, respectively.

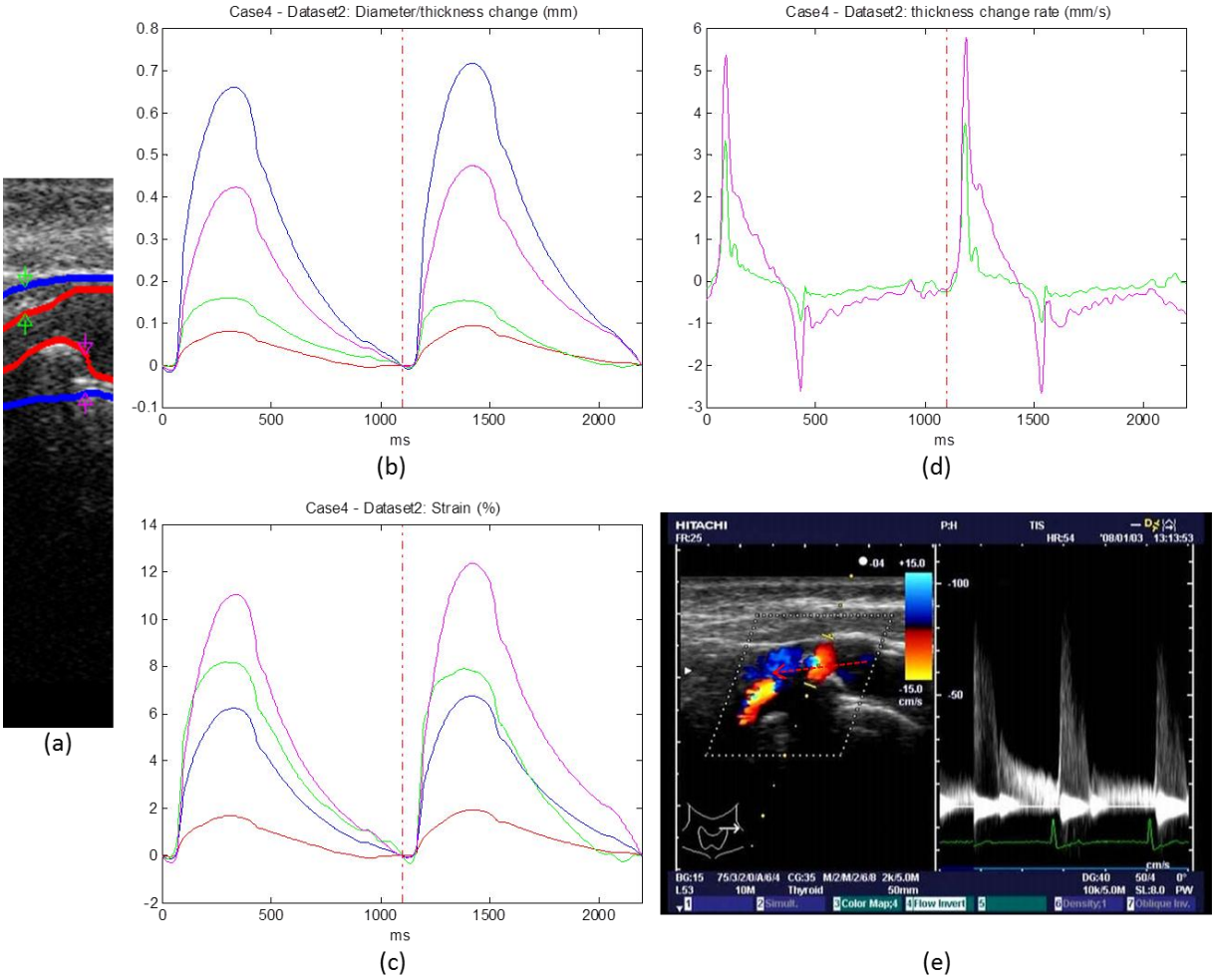

Figure 4-3. The arterial wall strain waveforms of another stenotic carotid segment. (a) The min-width BW frame with the arterial wall markers show stenotic plaques on both the near and the far walls of the artery; (b) The thickness change waveforms show inflation of both plaques (green and magenta); (c) The strain waveforms also indicate inflation of the plaques (green and magenta); (d) The thickness change waveforms show an increase in plaque inflation speed on both plaques; (e) The Doppler spectrum with a measured PSV of 85 cm/s and Doppler angle around 60 degree. The angle-adjusted PSV is 170 cm/s

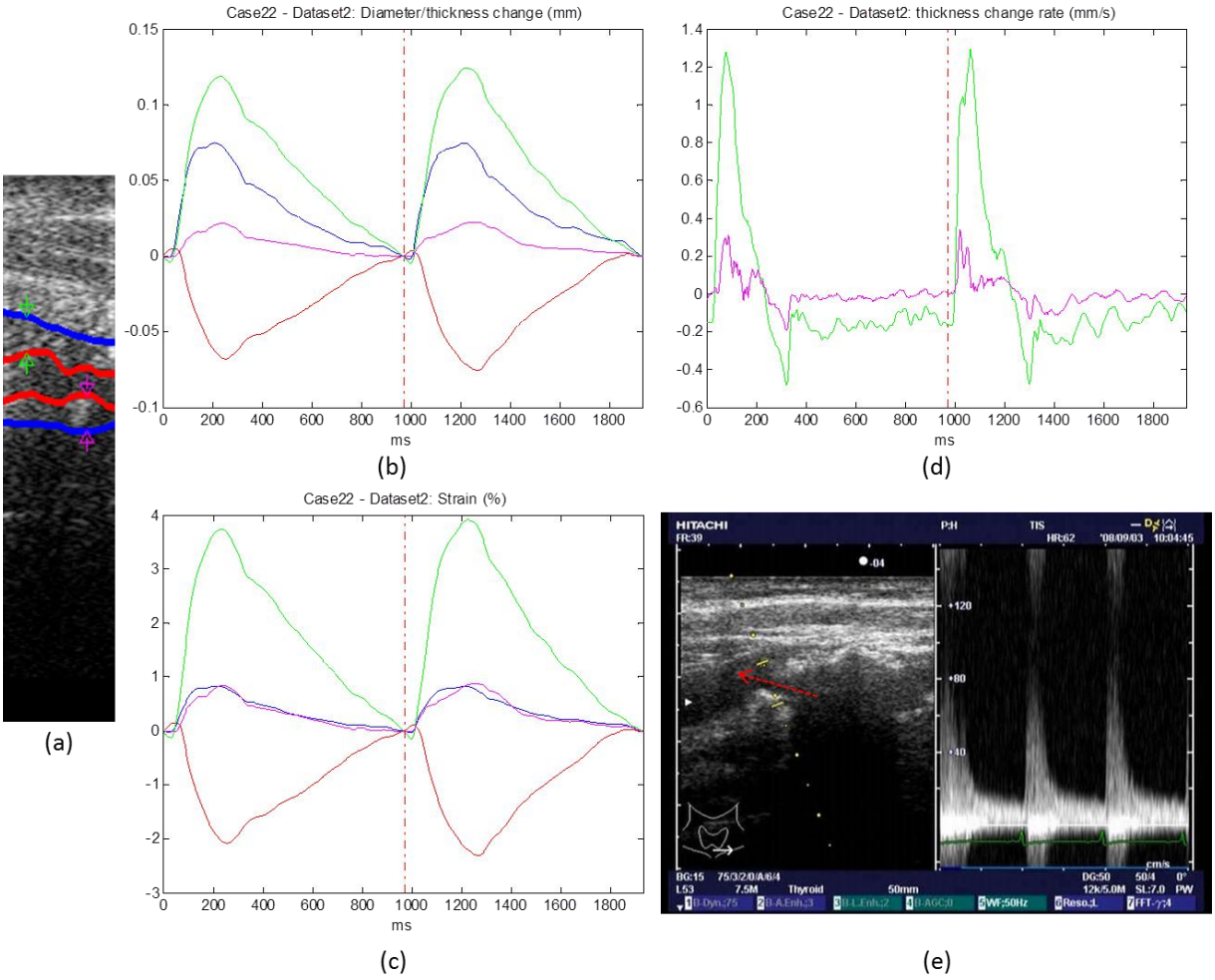

Figure 4-4. The arterial wall strain waveforms of a severely stenotic carotid segment. (a) The min-width BW frame with the arterial wall markers show great narrowing of the lumen due to the plaques on both the near and the far walls; (b) The thickness change waveforms show inflation of both plaques (green, magenta) and deflation of the lumen (red); (c) The strain waveforms also indicate inflation of the plaques (green and magenta); (d) The thickness change waveforms show an increase in plaque inflation speed on both plaque; (e) The Doppler spectrum: measured PSV – 80 cm/s, Doppler angle – 60 degree, angle-adjusted PSV – 160 cm/s.

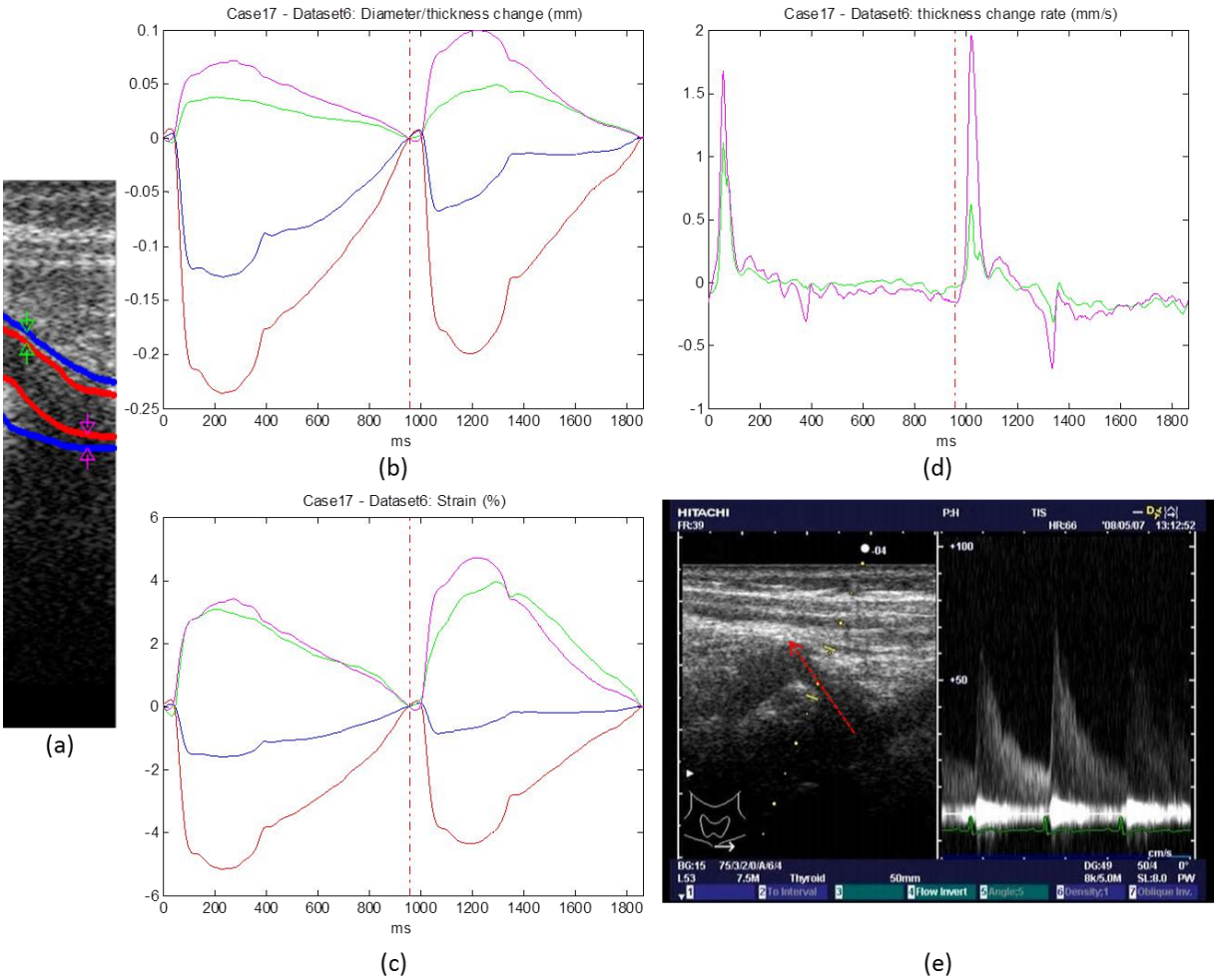

Figure 4-5. The arterial wall strain waveforms of another severely stenotic carotid segment. (a) The min-width BW frame with the arterial wall markers shows plaques on both the near and the far walls; (b) The thickness change waveforms show inflation of both plaques (green, magenta) and deflation of the lumen (red) and the outer wall (blue); (c) The strain waveforms also indicate inflation of the plaques (green and magenta) and the deflation of the arterial diameters; (d) The thickness change waveforms show an increase in plaque inflation speed on both plaque; (e) The Doppler spectrum, measured PSV – 70 cm/s, Doppler angle – 45 degree, angle-adjusted PSV – 100 cm/s

4.2 Plaque Inflation Metrics

Most of the plaques in the study exhibit a behavior of inflation. To quantify the inflation of plaque(s) in each case, several quantitative metrics were developed accordingly:

- *Max inflation* (unit: *mm*): the maximal value of the wall thickness change waveforms. The value could come from the near wall or the far wall, depending on which wall inflates more.
- *Max strain* (unit: *%*): the maximal value of the wall strain waveforms, from the near wall or the far wall, depending on which wall inflates more.
- *Max inflating rate* (unit: *mm/s*): the maximal value of the thickness change rate waveforms, from the near wall or the far wall, depending on which wall inflates faster.
- *Max deflating rate* (unit: *mm/s*): the minimal value (max negative) of the thickness change rate waveforms, representing the fastest deflating rate, from the near wall or the far wall, depending on which wall deflates faster.

In addition, two more metrics are introduced to estimate the absolute inflation of the plaque by taking the minimal thickness during the cardiac cycle as the reference, instead of the thickness at QRS:

- *Max abs inflation* (unit: *mm*): the difference between the maximum and minimum of the total wall thickness change waveforms, from the near wall or the far wall, depending on which wall inflates more.
- *Max abs strain* (unit: *%*): the percentage ratio to the minimum plaque thickness of the max inflation, from the near or far wall, depending on which wall inflates more.

Table 1 lists the values of the six metrics of all 22 cases, together with PSV and the percent stenosis. The cases with a high PSV (≥ 100 cm/s) have the PSV printed in bold, while the cases with a high stenosis (≥ 55%) also have the a bold stenosis value.

Table 1. The quantitative metrics and PSV of each case

Case number	*PSV* (*cm/s*)	*Stenosis (%)*	*Max inflation* (*mm*)	*Max strain* (*%*)	*Max inflating rate* (*mm/s*)	*Max deflating rate (-mm/s)*	*Max abs inflation (mm)*	*Max abs strain* (*%*)
1	78	**62**	0.103	3.3	0.98	1.11	0.172	5.7
2	44	**56**	0.060	2.6	0.61	0.46	0.069	3.0
3	**121**	50	0.127	0.9	0.49	1.10	0.052	2.4
4	**174**	**77**	0.474	12.3	5.78	2.66	0.486	12.7
5	**200**	**63**	0.115	4.4	2.95	2.11	0.119	4.5
6	**128**	50	0.126	5.8	2.91	1.68	0.142	9.6
7	**155**	20	0.038	3.4	0.80	1.87	0.110	10.7
8	78	**87**	0.011	0.4	0.14	0.33	0.025	1.8
9	**130**	**77**	0.093	4.5	0.81	1.34	0.164	8.1
10	**100**	54	0.058	2.1	0.76	1.38	0.200	10.6
11	60	43	0.017	2.1	0.70	0.60	0.064	4.5
12	60	37	0.050	3.9	1.01	0.83	0.106	8.7
13	40	44	0.037	2.6	0.75	1.25	0.092	3.9
14	40	29	0.043	3.6	0.39	0.85	0.061	5.1
15	**100**	41	0.086	4.6	1.37	0.89	0.174	9.9
16	60	38	0.015	0.8	0.36	0.29	0.022	1.6
17	**100**	**71**	0.154	3.2	2.80	1.04	0.163	9.8
18	60	**77**	0.054	2.2	0.39	0.53	0.060	2.5
19	**100**	**79**	0.087	3.8	2.25	1.80	0.215	13.4
20	80	46	0.198	7.9	3.36	0.87	0.209	8.4
21	80	**78**	0.143	4.8	3.50	1.19	0.145	4.8
22	**160**	**74**	0.124	3.9	1.30	1.69	0.196	9.6

If we divide all the 22 cases into two groups using a threshold of PSV (PSV >= 100 cm/s group and PSV <100 cm/s group), a two-sample t-test will show that the group with higher PSV has significantly higher values in three metrics: *max abs inflation* ($p < 0.05$), *max abs strain* ($p < 0.001$), and *max deflating rate* ($p < 0.001$). In the other three metrics, although it will fail to reject the null hypothesis, their *p*-value is still quite low (*max inflation*: $p = 0.17$; *max strain*: $p = 0.22$; *max inflating rate*: $p = 0.14$).

Figure 4-6 visualizes the relationship between each metric and PSV by plotting each metric with the corresponding PSV values as the x-axis. All the metrics display certain linear correlation with PSV. Their correlation coefficients are also calculated and displayed as the title of each sub

figure. Similarly, the relationship and correlation coefficient between the metrics and Bernoulli pressure drop, which is proportional to PSV^2, are shown in Fig. 4-7.

If using the percent stenosis as a threshold (>=55% group and <55% group), the two-sample t-test will not be able to reject the null hypothesis in any metric that the two groups are significantly different. The minimal *p*-value is 0.11 from max inflation. All the other metrics have a *p*-value greater than 0.2.

The plots between percent stenosis and each metric are shown in Fig. 4-8, together with their correlation coefficients on the title of each sub figure.

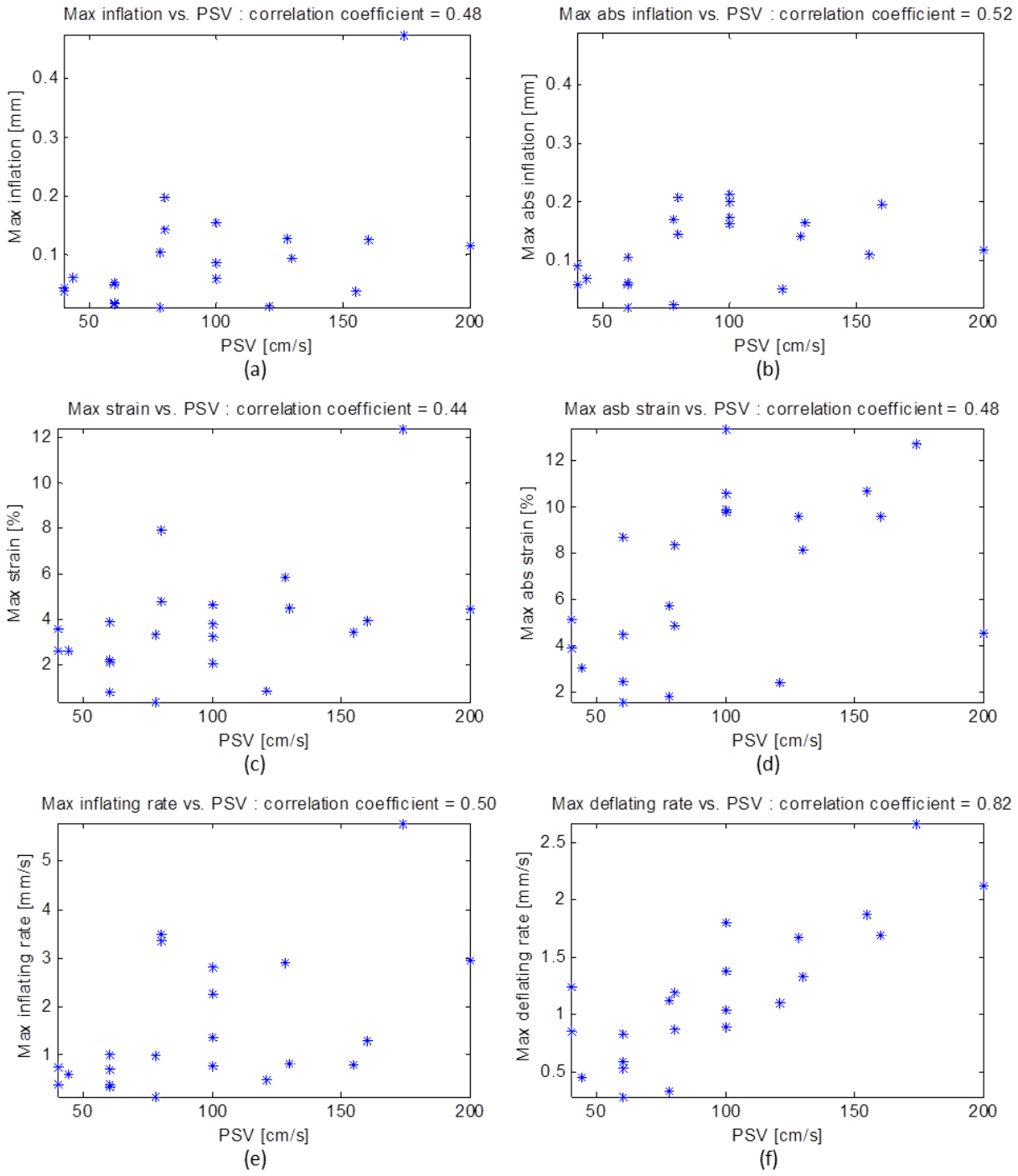

Figure 4-6. The relationship between the quantitative metrics and peak-systolic velocity (PSV): (a) max inflation with a correlation coefficient of 0.48; (b) max abs inflation with a correlation coefficient of 0.52; (c) max strain with a correlation coefficient of 0.44; (d) max abs strain with a correlation coefficient of 0.48; (e) max inflating rate with a correlation coefficient of 0.50; (f) max deflating rate with a correlation coefficient of 0.82

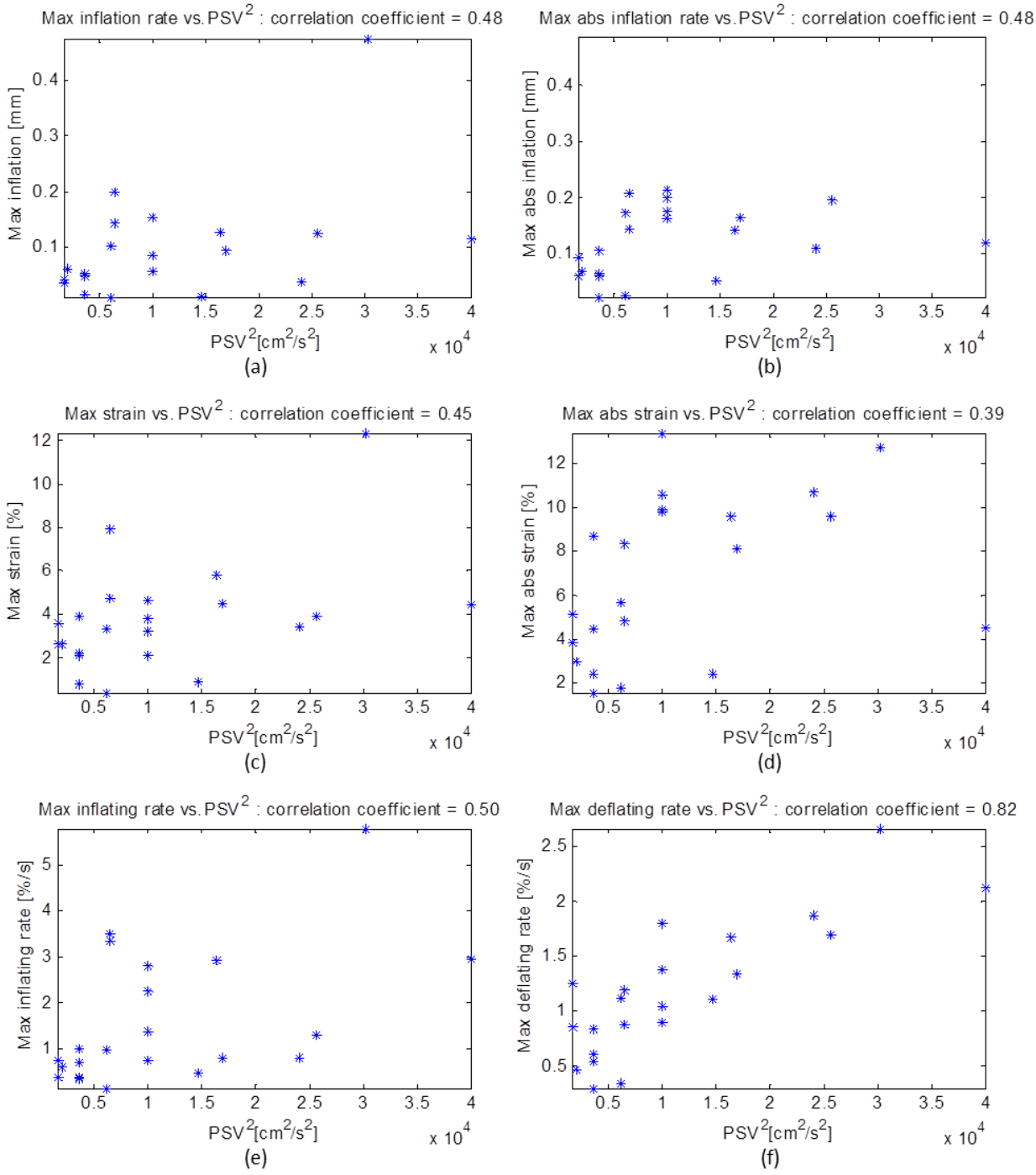

Figure 4-7. The relationship between the quantitative metrics and the Bernoulli pressure drop (PSV^2): (a) max inflation with a correlation coefficient of 0.48; (b) max abs inflation with a correlation coefficient of 0.48; (c) max strain with a correlation coefficient of 0.45; (d) max abs strain with a correlation coefficient of 0.39; (e) max inflating rate with a correlation coefficient of 0.50; (f) max deflating rate with a correlation coefficient of 0.82

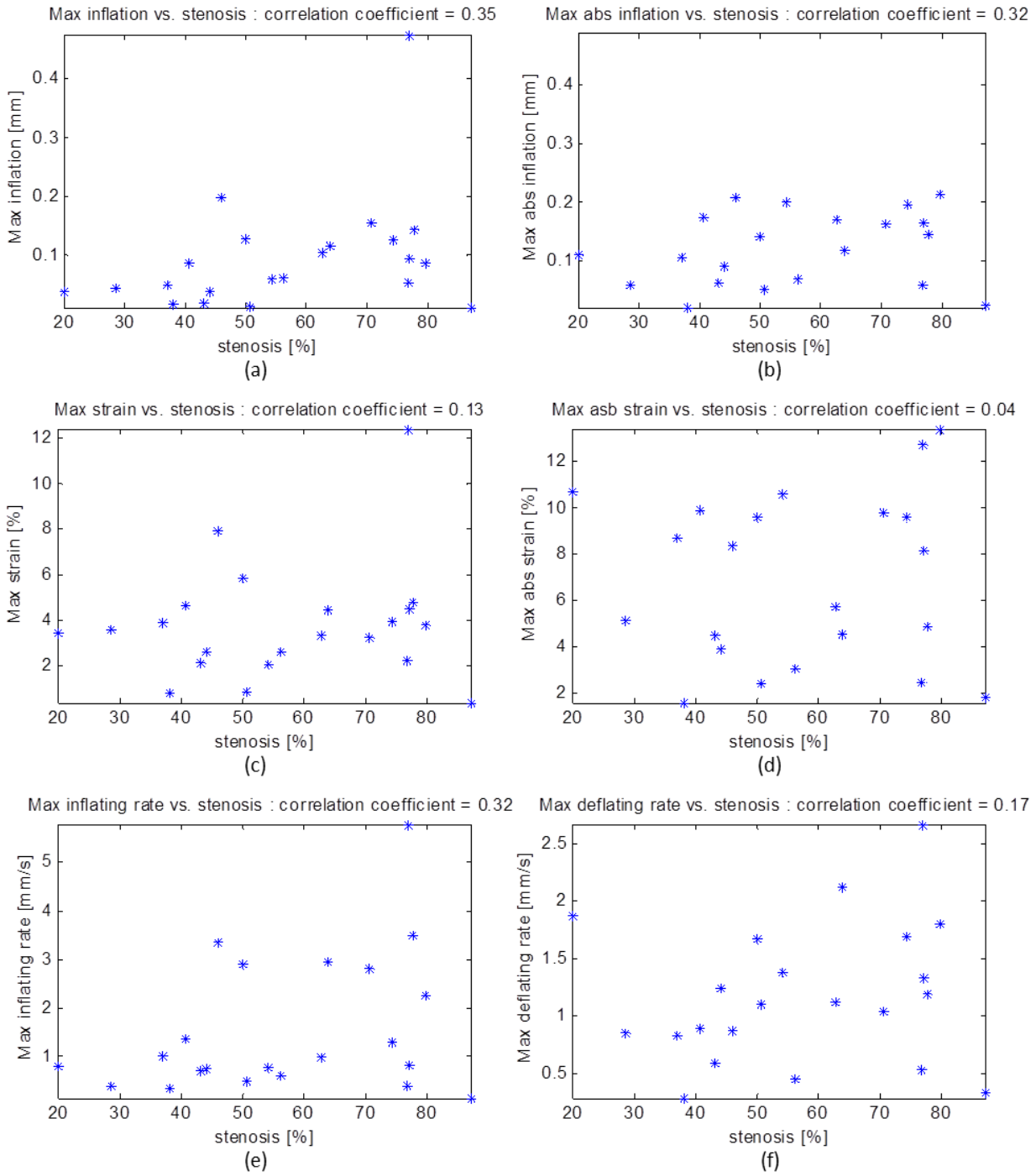

Figure 4-8. The relationship between the quantitative metrics and the percent stenosis: (a) max inflation with a correlation coefficient of 0.35; (b) max abs inflation with a correlation coefficient of 0.32; (c) max strain with a correlation coefficient of 0.13; (d) max abs strain with a correlation coefficient of 0.04; (e) max inflating rate with a correlation coefficient of 0.32; (f) max deflating rate with a correlation coefficient of 0.17

5 Discussion

5.1 The strain waveforms

The cyclic inflation of the carotid diameter should be proportional to the systematic pulsatile blood pressure cycles. In contrast, the change in thickness of normal vessel walls or the elastic plaques would be inversely proportional to the blood pressure waveform. For the normal vessel walls, increases in arterial diameter will enlarge the arterial circumference and hence reduce its average thickness. While for an elastic plaque, it is compressed more when the blood pressure is higher during systole. Therefore, its thickness change should also be inverted compared to the pressure change. This has been found in many datasets in our study, e.g., dataset 4 of case 13 (Fig. 4-1).

When VV are present inside the plaque to provide blood supply and pressure, the inflation of the plaque might not follow the normal pressure waveform inversely. Instead, it might exhibit some abnormal inflation patterns, likely due to the internal pressure from VV. Such phenomenon has been seen in most datasets with plaques. Some plaques even show an inflation waveform proportional to the pressure change, such dataset 2 of case 3 (Fig. 4-2) and dataset 2 of case 4 (Fig. 4-3). This might imply that the pressure of VV is also pulsatile and could be even higher than the one in the carotid lumen.

In some severe stenoses, the narrowing of blood lumen often results in higher peak-systolic velocity in blood when passing the stenosis. Due to the Bernoulli Effect, higher PSV causes pressure depression as some potential energy is converted to kinetic energy. Thus, a high PSV in systole is possible to make the systolic pressure even lower than the diastolic pressure around the stenosis. When that happens, we could observe a decrease in arterial diameter at systole, which

is opposite to the normal situation. This has been discovered in some cases, such as dataset 2 of case 22 (Fig. 4-4) and dataset 6 of case 17 (Fig. 4-5). Such pressure drop due to high PSV could pose a potential risk for plaque rupture.

5.2 Correlation between plaque metrics and PSV

The quantitative metrics for plaque inflation show moderate to good linear correlation with the PSV or PSV^2 which is proportional to the systolic pressure drop. There is no obvious difference between PSV correlation and PSV^2 correlation. In general, the performance of the absolute metrics, which are measured by taking the minimal plaque thickness as the reference point, is better than their counterparts with the thickness at QRS as the reference. This might be due to the pressure of VV not be the lowest at QRS, unlike the pressure in the lumen.

The metric of max inflating rate also shows good correlation as it is not influenced by accumulated bias. Surprisingly, the max deflating rate, describing how fast the plaque goes back to its original state after inflation, has the best correlation with PSV. Statistically, three of six metrics (two absolute metrics and the deflating rate) have significantly higher value when the PSV is high (>= 100 cm/s) with a significant level lower than 5%.

A moderate to good correlation between PSV and the plaque inflation metrics is reasonable since high PSV is not necessarily related to high density of VV. But PSV does affect the inflation of plaque through the Bernoulli Effect. In the future, we might need to combine the inflation metrics and PSV together to evaluate the vulnerability of plaques.

5.3 Correlation between plaque metrics and percent stenosis

By contrast, the correlation between the plaque inflation metrics and the percent stenosis is very weak. The results imply that they are almost independent. On the other hand, the correlation between PSV and percent stenosis is also very low (< 0.25). Although a larger plaque might have greater odds to have larger VV, severe stenosis does not necessarily mean higher PSV and larger pressure drop. This is probably due to the collateralization mechanism provide by the Circle of Wills [Henderson 2000] in the cerebral circulating system to compensate for the stenosis by deviating more blood flow to the carotid on the other side with no or less severe stenosis.

5.4 Limitation of the Study

As a pilot study on a smaller number of patients, it has several limitations to be overcome. First, only the 1-D strain in the axial direction is measured. However, the shape change of plaques could be in any direction. 1-D strain might not be accurate enough to measure the inflation of plaque precisely. Second, the flow patterns in the carotid bifurcation or around the stenotic region are usually very complicated. Helical, turbulent, jet, or reverse flows could be present there. Thus, conventional a Doppler spectrum with manual angle correction might not be able to accurately find the true PSV. Finally, lack of gold standards like MRI is still a basic limit of this study to objectively evaluate the inflation metrics.

5.5 Future direction

To continue from this pilot study to research on larger population, the following improvements could be considered.

First, 3D strain instead of 1D strain could be used. That requires a more advanced ultrasound system with advanced 2D matric probes [Konofagou 2000]. Also, vector Doppler should be adopted in the future study to accurately measure blood flow without any angular dependence [Dunmire 2000 and Jensen 2006]. That might require an updated ultrasound system as well. Moreover, we should consider collaboration between MRI labs to get the gold standards of VV.

6. Conclusion

Twenty-two atherosclerotic carotids from fourteen patients were studied with ultrasound strain imaging and spectral Doppler. The results show some plaques could inflate during the cardiac cycle, and the inflation has certain correlation with the peak-systolic velocity inside the carotid. The results provided preliminary evidence to support the hypothesis that intraplaque pressure from VV can inflate the plaque actively during cardiac cycles, and the increased peak-systolic velocity could increase the amount of plaque inflation by its Bernoulli Effect. This study has set up a foundation for future study on larger population.

7. Acknowledgements

I would like to thank all my committee members for their invaluable support for the completion of this master thesis. Especially, I want to thank Dr. Kirk Beach for his advice, encouragement and guidance during this project and during my entire graduate school period at UW Bioengineering.

I also want to thank Philips ultrasound, my current employer, for providing me the golden opportunity to grow not only in academia, but also in the real medical ultrasound industry. Philips also has been very supportive for me to complete my study at UW.

Finally and importantly, I would like to express my deep thanks to my family, especially my wife and my daughter, for their warm love and support during my study.

References

Beach KW, Hatsukami T, Detmer PR, Primozich JF, Ferguson MS, Gordon D, Alpers GE, Burns DH, BD Thackray, Strandness., "Carotid artery intraplaque hemorrhage and stenotic velocity", Stroke 1993, 24:314

Bo WJ, McKinney WM, and Bowden RL., "The Origin and Distribution of Vasa Vasorum at the Bifurcation of the Common Carotid Artery with Atherosclerosis", Stock 1989;20;1484

Carlier S, Kakadiaris IA, Dib N et al., "Vasa Vasorum Imaging: A New Window to the Clinical Detection of Vulnerable Atherosclerotic Plaques", Current Atherosclerosis Reports 2005, 7:164

Dunmire B, Beach KW, Labs KH, Plett M, Strandness DE., "Cross-beam vector Doppler ultrasound for angle-independent velocity measurements", Ultrasound in Med. & Biol. 2000, 26(8):1213

Gao L, Parker KJ, Lerner RM, Levinson SF, "Imaging of the elastic properties of tissue – a review", Ultrasound in Med. & Biol. 1996, 22(8):959

Go AS, Mozaffarian D, Roger VL et al., "Heart disease and stroke statistics--2013 update: a report from the American Heart Association", Circulation 2013, 127:e6-e245

Greenleaf JF, Fatemi M, Insana M., "Selected methods for imaging elastic properties of biological tissues", Annu. Rev. Biomed. Eng. 2003, 5:57

Hatle L, Brubakk A, Tromsdal A, Angelsen B., "Noninvasive assessment of pressure drop in mitral stenosis by Doppler ultrasound", Heart 1978, 40:131

Hatle L, Angelsen B. Tromsdal A., "Non-invasive assessment of aortic stenosis by Doppler ultrasound", Heart 1980, 43:284

Henderson RD, Eliasziw M, Fox AJ, Rothwell PM, Barnett HJM., "Angiographically defined collateral circulation and risk of stroke in patients with severe carotid artery stenosis", Stroke 2000, 31:128

Honda N, Matsumoto M. Maeda H, Hougaku H, Kamada T., "Ischemic Stroke Events and Carotid Atherosclerosis – Results of the Osaka Follow-up Study for UltraSonographic Assessment of Carotid Atherosclerosis", Stroke 1995, 26:1781

Jensen JA, Oddershede N, "Estimation of velocity vectors in synthetic aperture ultrasound imaging", IEEE transactions on medical Imaging 2006, 25(12):1637

Kampschulte A, Ferguson MS, Kerwin WS, Polissar NL, Chu B, Saam T, Hatsukami TS, Yuan C., "Differentiation of intraplaque versus juxtaluminal hemorrhage/thrombus in advanced human carotid atherosclerotic lesions by in vivo Magnetic Resonance Imaging", Circulation 2004, 110:3239

Konofagou EE, Ophir J, "Precision estimation and imaging of normal and shear components of the 3D strain tensor in elastography",Phys. Med. Biol. 1999, 45(6): 1553

Langheinrich AC, Kampschulte M, Buch T, Bohle RM, "Vasa vasorum and atherosclerosis – Quid novi?",Thromb Haemost 2007, 97:873

Naghavi M, Libby P, Falk E, et al., "From vulnerable plaque to vulnerable patient - a call for new definitions and risk assessment strategies: Part I",Circulation 2003, 108:1664

Rabben SI, Bjaerum S, Sorhus V, Torp H., "Ultrasound-based vessel wall tracking: an auto-correlation technique with RF center frequency estimation", Ultrasound in Med. & Biol. 2002, 28(4):507

Shamdasani V., "Noninvasive ultrasound elastography of atherosclerotic vascular disease: methods and clinical evaluation", *PhD dissertation* University of Washington 2007

Staub D, Schinkel AFL, Coll B et al., "Contrast-Enhanced Ultrasound Imaging of the Vasa Vasorum", JACC: Cardiovascular Imaging 2010, 3(7):761

Takaya N, Yuan C, Chu B, Saam T, Polissar NL, Jarvik GP, Isaac C, McDonough J, Natiello C, Small R, Ferguson MS, Hatsukami TS., "Presence of intraplaque hemorrhage stimulates progression of carotid atherosclerotic plaques: a high-resolution magnetic resonance imaging study", Circulation. 2005 May 31;111(21):2768

Virmani R, Kolodgie FD, Burke AP, Finn AV, Gold HK, Tulenko TN, Wrenn SP, Narula J., "Atherosclerotic plaque progression and vulnerability to rupture: angiogenesis as a source of intraplaque hemorrhage", Arterioscler. Thromb. Vasc. Biol. 2005 Oct;25(10):2054